Inorganic Chemistry

Communication

pubs.acs.org/IC

Magnetism of Linear $[Ln_3]^{9+}$ Oxo-Bridged Clusters (Ln = Pr, Nd) Supported inside a $[R_3PR']^+$ Phosphonium Coordination Material

Nolan W. Waggoner,[†] Beau Saccoccia,[†] Ilich A. Ibarra,[†,‡] Vincent M. Lynch,[†] Paul T. Wood,*[,§] and Simon M. Humphrey*[,†]

[†]Department of Chemistry, University of Texas at Austin, Welch Hall 2.204, 105 E. 24th Street A5300, Austin, Texas 78712-1224, United States

[§]University Chemical Laboratory, University of Cambridge, Lensfield Road, Cambridge CB2 1EW, United Kingdom

Supporting Information

ABSTRACT: Two new isostructural phosphine coordination materials, Ln-PCM-21 (Ln = Pr, Nd), have been obtained using a tris(*p*-carboxylated) methyltriphenylphosphonium ligand that is formally dianionic when triply deprotonated, allowing access to materials based on uncommon metal-to-ligand ratios. The polymers of the formula $[Ln_3(mptbc)_4]X{\cdot}solv$ (X = Cl^-, NO_3^-) are cationic and contain unusual, linear oxo-bridged $[Ln_3]^{9+}$ clusters. Magnetic susceptibility data for both the Pr and Nd analogues has been compared to models based on three contrasting approaches.

Lanthanide-based porous coordination polymer (PCP) materials hold a number of potentially beneficial advantages over transition-metal-based PCPs, but remain less common.[1] The expanded coordination number of Ln^{3+} ions and predominant ionic character of Ln−ligand bonding result in a range of coordination geometries, all with similar energies. Ln^{3+} ions tend to form PCPs with largely unpredictable network structures. However, the isolation of structurally well-characterized Ln^{3+} ions or clusters in ordered matrixes (e.g., PCPs) holds several advantages in terms of the resulting solid-state properties. For example, Ln-PCPs have been shown to be strongly luminescent because of tunable ligand-to-metal sensitization achieved via highly efficient ligand triplet to Ln^{3+} singlet nonirradiative energy transfer.[2] There have also been a number of recent examples of Ln-PCPs that can act as sensor materials for small-molecule adsorbates, achieved by monitoring of the relative luminescence quenching in response to particular adsorbates.[3]

The magnetic properties of Ln-based PCPs are another topical area of interest.[4] A major source of interest in the magnetic behavior of Ln^{3+} compounds arises from the expected differences from d-block metal species: not only are larger spin quantum numbers possible, but the lack of any covalency to the metal−ligand bonding does not quench the orbital contribution to the magnetic moment, thus making it possible to produce clusters with greater resulting magnetization.[4] Interest in Ln-containing species initially focused on mixed d−f species;[5] more recently, the discovery of single molecule magnet (SMM) behavior in Dy clusters,[5a,6] and in phthalocyanine sandwich compounds,[7] has shifted interest to homometallic Ln materials.

Our continued interest in the construction of Ln-PCPs using phosphine ligands (and derivatives thereof) for sensing applications has recently resulted in the isolation of an intriguing material that contains perfectly linear $[Ln_3]^{9+}$ trimers of Pr or Nd. The new phosphine coordination material Ln-PCM-21 was obtained as a crystalline solid by the direct reaction of a methyl triarylphosphonium chloride salt, $\{(H_3C)P(C_6H_4\text{-}p\text{-}CO_2)_3\}^{2-}$ ($mptcb^{2-}$; Scheme 1), with $Ln(NO)_3$ at 60 °C in a *N*,*N*-dimethylformamide/water/acetonitrile mixture. Isostructural materials could not be prepared with other Ln^{3+} ions, presumably indicating that formation of the material was highly sensitive to the cationic radius. The phosphonium chloride precursor $[mptbcH_3]Cl$ was obtained by reaction of the trilithium salt of phosphanotriylbenzenecarboxylic acid ($ptbcLi_3$; Scheme 1) with methyl iodide, followed by HCl workup. The resulting deprotonated tricarboxylate is pseudotetrahedral at the P atom and acts as a trigonal bridging group between adjacent metal clusters, which tends to greatly favor the formation of 3D polymers. The reduction of the overall charge on the tricarboxylate from 3− to 2− (due to the formal 1+ charge on P) seems to be important; it is not easy to obtain charge-neutral products based on simple $Ln^{3+}/mptbc^{2-}$ ratios. In fact, PCM-21 has the formula unit $[Ln_3(mptbc)_4]X{\cdot}solvent$, such that the framework is monocationic and X is a 1:1 mixture of Cl^- and NO_3^- anions [based on inductively coupled plasma mass spectrometry (ICP-MS), elemental analysis, and thermogravimetric analysis (TGA) data; see the Supporting Information (SI)].

Scheme 1. Preparation of the Phosphonium Chloride Precursor Used in Ln-PCM-21

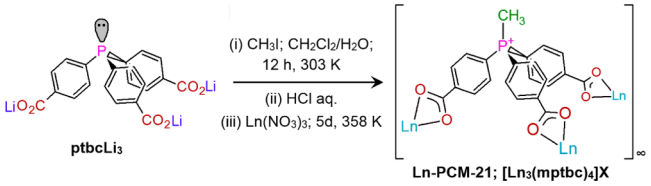

Single crystal X-ray diffraction of Nd-PCM-21 shows that it crystallizes in the rhombohedral space group $R\bar{3}c$ ($Z = 6$). There

Received: September 30, 2014
Published: December 3, 2014

are two crystallographically unique phosphonium ligands (Figure 1A) and two distinct Nd^{3+} sites. All carboxylate groups on both

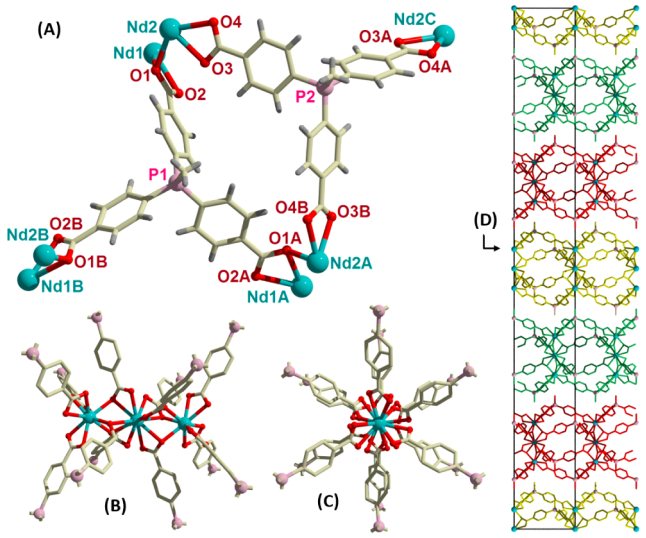

Figure 1. (A) Asymmetric unit of Nd-PCM-21. (B) View of one complete linear $[Nd_3]^{9+}$ trimer. P atoms (pink) are drawn with cutoff bonds to the other three substituents. (C) Alternative projection of the same $[Nd_3]^{9+}$ cluster along the Nd2−Nd1−Nd2 vector. (D) Unit cell of Nd-PCM-21 in the *bc* plane. The alternate orientations of each 2D sheet are colored in red, green, and yellow for clarity.

ligands chelate individual Nd^{3+} ions, with additional single atom−O bridges between adjacent Nd1 and Nd2 centers (Figure 1A). The ligands are near-tetrahedral at P, with bond angles of 108.6(2) and 109.1(3)°. The polymer network in Ln-PCM-21 takes the form of Ln_2P_2 rings that are fused to adjacent Ln_2P_2 rings at opposite corners by perfectly linear $[Ln_3]^{9+}$ clusters (Figure 1B,C). Each cluster consists of a central metal atom (Nd1) resident on a 6-fold site at (0, 0, 0), which is a 12-coordinate icosahedron due to 6-fold carboxylate chelation (Figure S2A in the SI); two 9-coordinate outer Nd2 sites with approximate monocapped square-antiprismatic coordination geometry (Figure S2B in the SI) complete each $[Ln_3]^{9+}$ trimer and are bridged to the central Nd1 site via three O1 atoms [2.447(5)−2.685(5) Å; Figure 1B]. The Nd1···Nd2 internuclear distance is 3.911(5) Å.

The extended structure contains stacked 2D bilayer sheets, in which there are six uniquely oriented layers that account for the very long *c* axis (104.37(3) Å, Figure 1D). Owing to the layered nature of the materials, they have modest Brunauer−Emmett−Teller surface areas of 121 and 132 $m^2\ g^{-1}$ (Pr and Nd, respectively; Figure S5 in the SI).

There are a growing number of reports of the magnetic properties arising from new types of Ln_x clusters supported inside molecular complexes and coordination polymers. Examples range from simple Ln_2 dimers[4,5,8] to isolated clusters of three or more Ln ions and infinite chains.[4,5,9] To the best of our knowledge, there is only one previous example of a linear Ln_3 cluster; a molecular $[Dy_3]^{3+}$ compound prepared using a tritopic pyridine bis(hydrazine) ligand scaffold was reported by Thompson and co-workers in 2012.[10] The magnetism of linear trimers are of particular interest because clusters with very high symmetry have fewer, more highly degenerate energy levels, which, in turn, reduces the number of magnetic relaxation pathways. Slow relaxation has also been eloquently demonstrated by Power and co-workers in the case of linear complexes of Fe^{2+} ions.[11]

The field-cooled magnetic susceptibility of both Pr- and Nd-PCM-21 (external field of 100 Oe) showed continuously increasing susceptibility with decreasing temperature and no sign of any discontinuity, which indicates that there is no long-range order down to 5.0 K (Figures S6 and S7 in the SI). The high-temperature data for both samples could be fitted to the Curie−Weiss law and gave reasonable values for ions with $^3H_4$ and $^4I_{9/2}$ ground states for Pr^{3+} and Nd^{3+}, respectively.

From a magnetic perspective, each trimer in Ln-PCM-21 can be simplified, as shown in Figure 2: the only potential

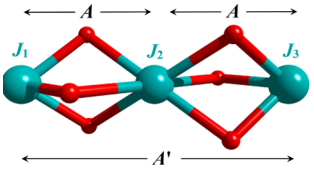

Figure 2. Simplified magnetic model and potential coupling constants for the individual $[Ln_3]^{9+}$ clusters in Ln-PCM-22.

superexchange pathways between adjacent Ln^{3+} sites are provided by three single atom carboxylate−O bridges. Because the metal−ligand bonding is mostly ionic, actual orbital overlap within the Ln−O−Ln bridges is expected to be minimal; thus, the electron orbital momentum should remain unquenched. Therefore, *J* values ($J = L + S$, $(L + S) - 1$, ..., $|L - S|$) are the appropriate quantum numbers to consider (rather than *S* itself). The Pr^{3+} and Nd^{3+} materials have negative Weiss constants of −64(3) and −42(1) K, respectively (Figures S7 and S8 in the SI). Plots of $\chi_m T$ vs *T* for both analogues were consistent with the observed negative Weiss constant, and the high temperature values are consistent with derived Curie constants (Figure 3).

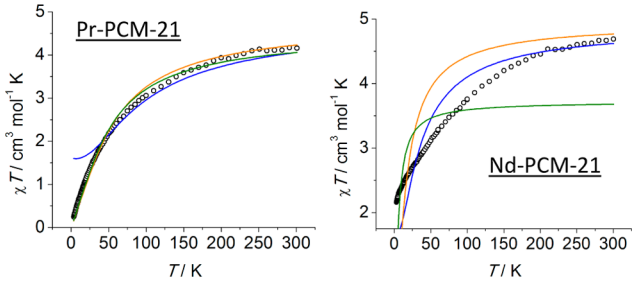

Figure 3. Plots of observed $\chi_m T$ versus *T* (black circles) and the three models examined (superexchange model, blue line; ZFS model, orange line; ZFS + MFT, green line).

Three possible causes of deviation from pure Curie law behavior have to be considered; exchange interaction between neighboring ions, thermal population of excited states within the ^3H and ^4I manifolds, and tetragonal zero-field splitting (ZFS) of the $J = 4$ and $^9/_2$ ground terms into $m_J = 4, 3, 2, 1, 0$ and $^9/_2$, $^7/_2$, $^5/_2$, $^3/_2$, $^1/_2$ states. In the case of these two ions, thermal population of excited *J* states should always give rise to greater magnetization and, therefore, a positive Weiss constant. Population of even the lowest-energy excited states further be ruled out because the magnitude of the spin−orbit coupling constants for Pr^3 and Nd^{3+} (λ = 400 and 350 cm^{-1}) give rise to first-excited-state energy gaps of 576 and 432 K (400 and 450 cm^{-1}), respectively.

We then attempted to model the magnetic behavior in three different ways: (1) by assuming that superexchange is the only

dx.doi.org/10.1021/ic5023642 | Inorg. Chem. 2014, 53, 12674−12676

important factor; (2) by considering only the effect of ZFS; (3) by adding a small magnetic coupling perturbation onto the ZFS model via an additional mean-field-theory (MFT) term (see the SI). Superexchange was modeled by consideration of the isotropic spin Hamiltonian (eq S1), and using Kambé vector coupling to derive an expression for the energies of the possible spin states (eq S2). Resulting in expressions with 61 (Pr) and 75 (Nd) states. ZFS produces states with energies equal to $D(m_J)^2$ and an overall magnetic susceptibility per $[Ln_3]^{9+}$ given by eq S3. This expression can be further modified to account for magnetic interactions that are much smaller than the effect of ZFS using eq S4.[12]

The lack of appreciable metal-ligand covalency should result in weak magnetic exchange as observed for other Ln clusters.[13] If superexchange is indeed the most important factor, $\chi_m T$ should remain close to its limiting high-temperature value with decreasing T. This would, in turn, indicate that the thermal energy is still much larger than the strength of the exchange interaction. In the observed data, $\chi_m T$ began to decay quite quickly but then remained higher than predicted at very low T. This is in line with observations in previous studies.[14] eq S2 yielded reasonable values for the coupling constant, $A = -2.8(3)$ cm^{-1} for Pr-PCM-21 and $-0.80(4)$ cm^{-1} for Nd-PCM-21, but did not give a satisfactory fit across the entire temperature range for either compound (blue fit, Figure 3A,B). Next, the effect of tetragonal ZFS was considered. This gave a much better result for Pr-PCM-21 [orange fit, Figure 3A; $D = 7.2(1)$ K and $R^2 = 0.990$] and was further improved by considering the additional effect of MFT [green fit, Figure 3A; $D = 6.8(1)$ K, $A = -0.012(2)$ K, and $R^2 = 0.993$]. In contrast, the data for Nd-PCM-21 could not be fitted as well using ZFS [orange fit, Figure 3B; $D = 1.7(1)$ K and $R^2 = 0.049$] and was only marginally improved using the ZFS + MFT approach [green fit, Figure 3A $D = 0.73(7)$ K, $A = -0.0$ K, and $R = 0.530$]. It is unlikely that interlayer dipolar coupling plays any role in the observed magnetism because the nearest $Ln^{3+}\cdots Ln^{3+}$ distances are well separated (12.6 Å) and through-space coupling falls off quickly with increasing separation. A rationalization for the inability to accurately model the behavior of the Nd material can be found from electron paramagnetic resonance studies, which have shown that Pr^{3+} has an approximate tetragonal splitting as modeled[15] but that the anisotropy of Nd^{3+} ions is distinctly rhombic[16] and therefore requires a more complex model.

■ ASSOCIATED CONTENT

Supporting Information

X-ray crystallographic data in CIF format, syntheses of Ln-PCM-22 materials, ^1H and ^{31}P NMR and Fourier transform infrared spectra, ICP-MS, elemental analyses, powder X-ray diffraction patterns, TGA data, gas sorption/desorption isotherms, luminescence spectra, and equations and a description of the magnetic modeling methods employed. This material is available free of charge via the Internet at http://pubs.acs.org.

■ AUTHOR INFORMATION

Corresponding Authors

* E-mail: ptw22@cam.ac.uk.
* E-mail: smh@cm.utexas.edu.

Present Address

‡I.A.I.: Instituto de Investigaciones en Materiales, Universidad Nactional Autónoma de México.

Notes

The authors declare no competing financial interest.

■ ACKNOWLEDGMENTS

We thank the Welch Foundation (Grant F-1738) for financial support of this work.

■ REFERENCES

(1) Chen, Y.; Ma, S. *Rev. Inorg. Chem.* **2012**, *32*, 81−100.

(2) (a) Kreno, L. E.; Leong, K.; Farha, O. K.; Allendorf, M.; Van Duyne, R. P.; Hupp, J. T. *Chem. Rev.* **2012**, *112*, 1105−1125. (b) Cui, Y.; Yue, Y.; Qian, G.; Chen, B. *Chem. Rev.* **2012**, *112*, 1126−1162. (c) Rocha, J.; Carlos, L. D.; Paz, A. A. A.; Ananias, D. *Chem. Soc. Rev.* **2011**, *40*, 926−940.

(3) For example, see: (a) Kuppler, R. J.; Timmons, D. J.; Fang, Q.-R.; Li, J.-R.; Makal, T. A.; Yound, M. D.; Yuan, D.; Zhao, D.; Zhuang, W.; Zhou, H.-C. *Coord. Chem. Rev.* **2009**, *253*, 3042−3066. (b) Cui, Y.; Xu, H.; Yue, Y.; Guo, Z.; Yu, J.; Chen, Z.; Gao, J.; Yang, Y.; Qian, G.; Chen, B. *J. Am. Chem. Soc.* **2012**, *134*, 3979−3982. (c) White, K. A.; Changelis, D. A.; Gogick, K. A.; Stehman, J.; Rosi, N. L.; Petoud, S. *J. Am. Chem. Soc.* **2009**, *131*, 18069−18071. (d) Ibarra, I. A.; Hesterberg, T. W.; Chang, J.-S.; Yoon, J.-W.; Holliday, B. J.; Humphrey, S. M. *Chem. Commun.* **2013**, *49*, 7156−7158.

(4) Woodruff, D. N.; Winpenny, R. E. P.; Layfield, R. A. *Chem. Rev.* **2013**, *113*, 5110−5148.

(5) (a) Sessoli, R.; Powell, A. K. *Coord. Chem. Rev.* **2009**, *253*, 2328−2341. (b) Layfield, R. A. *Organometallics* **2014**, *33*, 1084−1099.

(6) (a) Tang, J.; Hewitt, I.; Madhu, N. T.; Anson, C. E.; Powell, A. K. *Angew. Chem., Int. Ed.* **2006**, *45*, 1729−1733. (b) Long, J.; Habib, F.; Lin, P. O.; Korobkov, I.; Enright, G.; Ungur, L.; Wernsdorfer, W.; Chibotaru, L. F.; Murugesu, M. *J. Am. Chem. Soc.* **2011**, *133*, 5319−5328.

(7) Fukada, T.; Natsuko, S.; Yamamura, T.; Ishikawa, N. *Inorg. Chem.* **2014**, *53*, 9080−9086.

(8) (a) Su, S.; Wang, S.; Song, X.; Sing, S.; Qin, C.; Zhu, M.; Hao, Z.; Zhao, S.; Zhang, H. *Dalton Trans.* **2012**, *41*, 4772−4779. (b) Bhunia, A.; Lan, Y.; Mereacre, V.; Gamer, M. T.; Powell, A. K. *Inorg. Chem.* **2011**, *50*, 12697−12704. (c) Manolis, M. J.; Kyprianidou, E. J.; Papaefstathiou, G. S.; Tasiopoulos, A. J. *Inorg. Chem.* **2012**, *51*, 6308−6314. (d) Setyawati, I. A.; Liu, S.; Rettig, S. J.; Orvig, C. *Inorg. Chem.* **2000**, *39*, 496−507.

(9) (a) Jami, A. K.; Baskar, V.; Sañudo, E. C. *Inorg. Chem.* **2013**, *52*, 2432−2438. (b) Fang, W.-H.; Cheng, L.; Huang, L.; Yang, G.-Y. *Inorg. Chem.* **2013**, *52*, 6−8. (c) Singh-Wolmit, M. A.; Sinclair, R. A.; Andrews, M.; Rowland, C.; Cahill, C. L.; Murugesu, M. *Polyhedron* **2013**, *53*, 187−192.

(10) Anwar, M. U.; Tandon, S. S.; Dawe, L. N.; Habib, F.; Murugesu, M.; Thompson, L. K. *Inorg. Chem.* **2012**, *51*, 1028−1034.

(11) (a) Zadrozny, J. M.; Atanasov, M.; Bryan, A. M.; Lin, C.-Y.; Rekken, B. D.; Power, P. P.; Neese, F.; Long, J. R. *Chem. Sci.* **2013**, *4*, 125−138. (b) Zadrozny, J. M.; Xiao, D. J.; Atanasov, M.; Long, G. J.; Grandjean, F.; Neese, F.; Long, J. R. *Nat. Chem.* **2013**, *5*, 577−581.

(12) Zhang, X.; Xu, N.; Yang, S. Y.; Zhao, X. Q.; Cheng, P. *RSC Adv.* **2014**, *4*, 40643−40650.

(13) Zhou, X.; Xia, S.; Tanner, P. A. *J. Phys. Chem. B* **2007**, *111*, 8677−8685.

(14) (a) Legendziewicz, J.; Keller, B.; Turowska-Tyrk, I.; Wojciechowski, W. *New J. Chem.* **1999**, *23*, 1097−1103. (b) Cepeda, J.; Balda, R.; Beobide, G.; Castillo, O.; Fernandez, J.; Luque, A.; Perez-Yanez, S.; Roman, P.; Vallejo-Sanchez, D. *Inorg. Chem.* **2011**, *50*, 8437−8451.

(15) Kaczmarek, S. M.; Tomaszewicz, E.; Mosznynski, D.; Jasik, A.; Leniec, G. *Mater. Chem. Phys.* **2010**, *124*, 646−651.

(16) Mingalieva, L. V.; Voronkova, V. K.; Galeez, R. T.; Sukhanov, A. A.; Melnik, S.; Prodius, D.; Turta, K. I. *Appl. Magn. Reson.* **2010**, *37*, 737.